Journal of
Renewable Energy Research and Applications (RERA)

Vol. 6, No. 2, 2025, 259-268 *DOI: 10.22044/rera.2025.16116.1418*

Experimental Analysis of a Silica Gel–Water Adsorption Cooling System with Integrated Chamber for Adsorbent Bed and the Condenser

A. Fahim, A. Nazari, M. Zamen*, A. Salamat Asrami

Faculty of Mechanical Engineering, Shahrood University of Technology, Shahrood, Iran.

Received Date 28 April 2025; Revised Date 26 June 2025; Accepted Date 29 September 2025
**Corresponding author: zamen@shahroodut.ac.ir (M. Zamen)*

Abstract
A significant portion of energy consumption, particularly during the summer, is attributed to cooling demands in buildings. The most common methods for providing cooling are vapor compression and absorption refrigeration systems. However, in recent years, alternative methods based on adsorption have been explored, and some systems have even reached the commercial market. In Iran, however, such systems have only been investigated at the laboratory level. The goal of this experimental study is the evaluation of a silica gel–water adsorption cooling system. The constructed system included an adsorbent bed filled with silica gel, a condenser, an evaporator, a heating unit, and a cooling water circulation system. A key feature of this design is the use of a chamber for both the adsorbent bed and the condenser which makes the system simpler. After construction, the system was tested and its performance data were collected. The cooling energy produced at the end of each cycle was measured based on the temperature change in the evaporator. According to the results, the cooling energy per cycle ranged between 1.3 and 1.8 kWh, with a maximum heating energy requirement of approximately 1.8 kWh. Based on various experimental runs, the coefficient of performance (COP) of the system was calculated to be in the range of 0.035 to 0.048. The use of an integrated chamber simplifies the system, but it results in reduced performance.

Keywords: *Refrigeration, Adsorption, Silica Gel, Coefficient of Performance.*

1. Introduction

Energy scarcity is one of the most critical challenges facing humanity, and it is expected to cause serious problems in the near future [1]. Energy has various applications, including transportation, heating, cooling, and electricity production. Among these, cooling is essential for providing thermal comfort and reducing temperature during hot seasons. Cooling can be achieved through various means such as electrical and mechanical devices, employing different methods [2]. Absorption cooling systems are generally classified into two types: absorption and adsorption systems. The main difference between absorption and adsorption chillers lies in the nature of the adsorbent material. In absorption chillers, the adsorbent is in liquid form, and the refrigerant is absorbed volumetrically. In contrast, adsorption chillers use solid adsorbents, and the refrigerant is adsorbed on the surface [3]. The four main components of an adsorption chiller are the adsorber chambers, condenser, evaporator, and expansion valve. Industrial applications typically utilize two adsorber chambers in the system. Although the concept of solid-based adsorption cooling has been known for a long time, its application in building cooling systems is relatively recent, with the first commercial model introduced in 1986. In such systems, water serves as the refrigerant, while silica gel functions as the adsorbent [4]. The heat required for the regeneration of the adsorbent is usually supplied by hot water ranging from 55°C to 90°C, and the outlet chilled water temperature can be reduced to as low as 3.3°C [5]. Several studies have been conducted in this field. Razek et al. [6] carried out both theoretical and experimental investigations on silica gel–water refrigeration systems. A Dynamic Vapor Sorption (DVS) analyzer was used to evaluate a new class of adsorbents known as Metal–Organic Frameworks (MOFs). These adsorbents exhibit high water adsorption potential and could serve as replacements for conventional silica gel. MOFs were characterized in terms of adsorption isotherms and kinetics, as well as their performance in cyclic operations. It was found that HKUST-1, a copper-based MOF, showed a

95.7% increase in water uptake compared to silica gel. Additionally, an iron-based MOF demonstrated better performance than silica gel under high evaporation temperature conditions.

Younes et al. [7] investigated an adsorption chiller using silica gel for cooling applications. They also examined the porous properties and thermal conductivity of thermal composites, concluding that the thermal conductivity of the prepared composites was approximately 2.8 times higher than that of silica gel powder. Pan et al. [8] studied a 3 kW adsorption chiller utilizing silica gel and water. Their results indicated that the system could achieve a cooling capacity of 3.98 kW with a coefficient of performance (COP) of up to 0.632. The optimal half-cycle time was determined to be 750 seconds. Additionally, the outlet temperature of the cooling water reached 39.9°C, making it suitable for domestic hot water applications. Manila et al. [9] analyzed a two-stage adsorption chiller using silica gel and water vapor. They examined the influence of critical bed depth and silica gel particle size on adsorption. Their results showed that both cooling capacity and COP were dependent on ambient temperature, and an optimal particle diameter for silica gel was identified. Carroll et al. [10] investigated the effect of adhesives used in the production of adsorption beds to enhance heat transfer on the target surface. Experiments were conducted using silica gel and three types of adhesives on metal heat exchanger plates. The results indicated that samples using hydroxyethyl cellulose adhesive exhibited lower moisture adsorption capacity. Lee et al. [11] evaluated the performance of an adsorption chiller system using three different adsorbents—silica gel, aluminum fumarate, and 01FAM-Z—to assess the impact of adsorption isotherms and physical characteristics. Their findings showed that among the three tested adsorbents, 01FAM-Z delivered the best performance, with a coefficient of performance (COP) of 5.13. Liu et al. [12] studied the performance of a solar-powered adsorption cooling system utilizing silica gel and the zeolite SAPO-34. Experimental results showed that the system achieved maximum performance at an adsorption time of 45 minutes, with a COP of 0.258. Furthermore, a comparative analysis between the optimal performance of the silica gel system and the SAPO-34 system revealed that cooling capacity and COP for the silica gel system were highly dependent on adsorption time. At optimal adsorption conditions, the COP of the silica gel system was 1.93 times greater than that of the SAPO-34 system. Overall, the silica gel–water pair demonstrated superior performance compared to the SAPO-34 zeolite–water pair in solar adsorption cooling applications. Naja et al. [12] conducted an experimental analysis of the adsorption refrigeration cycle using a solar-powered system with the silica gel–water pair. Compared to other adsorbents (such as activated carbon–methanol and zeolite–water), silica gel–water offers superior physical and thermal properties of water (high latent heat of vaporization, low viscosity, high thermal conductivity, and thermal stability) across a wide range of conditions. Di et al. [13] carried out theoretical and experimental studies on the performance characteristics of a newly designed silica gel–water chiller under variable heat source temperatures. Their findings revealed that the COP is significantly influenced by the rate of temperature variation in the heat source. The results also suggested that when powered by solar energy, the system should incorporate a buffer tank to enhance performance during low solar radiation periods. However, using a buffer during periods of high solar radiation may lead to unnecessary electrical energy consumption and result in a lower COP. Thomas et al. [14] developed an adsorption chiller and heat pump system for residential heating and air conditioning applications. The results of two prototypes indicated promising advancements. The heating COP exceeded 1.5, while cooling COPs for air conditioning purposes (12–15°C) reached up to 0.5. The device is being developed for the small-capacity chiller market, with a nominal cooling capacity range of 3–8 kW and a nominal heating capacity of up to 16 kW. While silica gel as an adsorbent is suitable at 75°C, the improved design also allows for the use of other adsorbents such as zeolites when higher temperatures are available. Chen et al. [15] studied a water–silica gel adsorption chiller without a vacuum valve. Their findings showed that when the average inlet hot water temperature, inlet cooling water temperature, and outlet chilled water temperature were 82.0°C, 31.6°C, and 12.3°C respectively, the cooling capacity and COP reached 9.60 kW and 0.49, respectively. Chorowski et al. [16] modeled and experimentally examined an adsorption chiller using low-grade waste heat from cogeneration. The study presented a thermodynamic model of a triple-bed adsorption chiller with a cooling capacity of 90 kW. The system provided cooling at two temperature levels—approximately 13°C and 8°C. The dependence of the chiller's COP on the adsorption bed regeneration temperature was identified

within the range of 45°C to 70°C. The system could be operated using hot water at 65°C, which corresponds to typical cogeneration heating conditions in distributed systems. Pan et al. [17] carried out an experimental study on an adsorption chiller designed to utilize low-temperature waste heat. For application in data centers, the chiller was tested under operating conditions of 51.4°C to 61.3°C, achieving a COP between 0.285 and 0.477, while producing chilled water at 18.8°C to 22.4°C. These experimental results confirm the feasibility and strong performance of the water–silica gel adsorption chiller for low-grade waste heat recovery applications. Pan et al. [18] conducted experimental research on an adsorption chiller designed to utilize low-grade waste heat. In scenarios using data center waste heat (51.4–61.3°C), the chiller achieved COPs ranging from 0.285 to 0.477 while producing chilled water at 18.8–22.4°C. These findings confirmed the feasibility and reliable performance of silica gel–water chillers in low-temperature waste heat recovery applications. Sah et al. [19] conducted a comparative experimental analysis of two adsorption cooling systems using silica gel/water and silica gel/methanol pairs under waste heat conditions in the range of 60–90 °C. Their results showed that the silica gel/water pair exhibited superior performance at higher driving temperatures, achieving a coefficient of performance (COP) of approximately 0.45 and a specific cooling power (SCP) of nearly 100 W/kg, indicating its suitability for applications utilizing mid-temperature waste heat. In another study, El-Ghetany et al. [20] designed and simulated a solar-powered adsorption chiller using the silica gel/water pair for air conditioning applications. The system was modeled using MATLAB/Simulink and analyzed for cooling loads ranging from 10 to 100 TR. The study reported a COP of up to 0.55 and emphasized the potential of solar thermal energy, especially with solar concentrators, to significantly enhance the system's thermal performance and reliability. Complementing these studies, Du et al. [21] developed and experimentally tested a compact silica gel/water adsorption cooling unit intended for data center cooling powered by industrial waste heat. Their prototype demonstrated a COP of around 0.43 under a driving temperature of 85 °C, with improved heat exchange due to the compact design and reduced thermal resistance.

In this study, an adsorption cooling system has been practically tested. By reviewing previous studies, it was found that most of the systems built have separate chambers for the condenser, evaporator and absorber bed. The most important feature of the design examined in this study is the use of a chamber for both the adsorbent bed and condenser. In this way, the complexity of the system can be reduced. In this experimental study, the use of this chamber has been investigated.

2. Process description

The schematic of the system developed in this study is shown in figure 1. As can be observed, the bed containing silica gel and the condenser are placed within a chamber. The evaporator is located outside the chamber, with an inlet and an outlet.

The connection between the different sections is controlled using separate valves. If the silica gel bed is saturated with water, first the hot water valve is opened and the hot water passes through the absorbent bed and desorption process is started. Water evaporated and the chamber pressure increases. After the pressure reaches a certain level, the condenser valve is opened and the process of condensation of water vapor in the chamber takes place simultaneously with the passage of cold water through the condenser. The condensed water is directed to the evaporator from the pipe under the bed, which is connected to the evaporator. When the chamber cooling operation is completed, the connection valve to the evaporator is opened and, given that the evaporator pressure is lower, the evaporation process is carried out in the evaporator. The required heat for evaporation supplies from the water in the evaporator tank and causes it to cool. On the other hand, cold water flows into the bed and cools it and is ready for the absorption process. After the bed cools, by opening the upper valve between the evaporator and main chamber, water vapor flows into the chamber and re-absorbs the bed. This process can continue continuously.

Since silica gel is used as the adsorbent in this study, an initial description of its characteristics and sourcing is provided. Silica gel is a solid material composed of silicon dioxide (SiO_2), known for its porous structure and high porosity, which gives it excellent adsorption capability. It is non-flammable and can absorb up to 40% of its own weight in moisture. This compound does not cause corrosion or degradation of materials, is easy to package, and is available in various sizes for different applications. When stored in a dry, moisture-free environment, silica gel has an unlimited shelf life. It is non-toxic, odorless, and exhibits highly stable thermal and chemical

properties. Additionally, it maintains its physical appearance even after absorbing moisture. After absorbing moisture, silica gel must either be replaced or regenerated. To regenerate silica gel for reuse, it should be dried by indirect heating at approximately 60-150°C. Direct exposure to heat or prolonged heating may burn the silica gel and impair its adsorption properties. When properly stored and kept away from ambient moisture, silica gel can be reused.

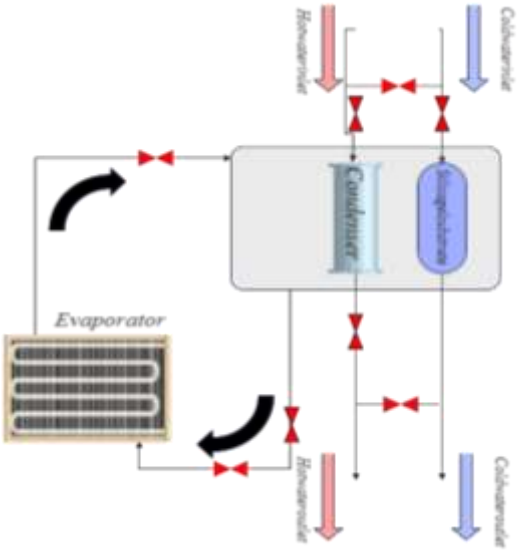

Figure 1. Schematic of the cycle used.

Figure 2. Samples of silica gel.

3. System description

The main part of the system is the chamber that contains absorbent bed and condenser. For both of them, a type of fin-tube heat exchanger is used. In the adsorbent bed, silica gel is held on the outer surface of one of the exchangers by a mesh. As shown in figure 3, The condenser is also located next to the absorber.

Figure 3. The condenser used in this study.

An evaporator is a device that continuously absorbs heat from the surrounding environment, where the refrigerant undergoes phase change through evaporation. In the evaporator, the temperature of the space or substance being cooled must always be higher than that of the refrigerant to allow for effective heat transfer. Therefore, in a refrigeration cycle, any component in which the refrigerant evaporates during the cooling process is referred to as an evaporator. In this study, to enhance efficiency, the evaporator was placed inside an insulated tank (Figure 4). Table1 presents the other equipment used in the system. A powerful vacuum pump was also used to create a vacuum throughout the system (Figure 5).

Figure 4. The evaporator used in this study.

Table 1. Other equipment used in the study.

Row	Equipment	Description
1	Circulation Pump	A 500-watt pump was used to circulate and pump water through the system.
2	Vacuum Pump	The vacuum pump is a device used to create a vacuum for various applications. This vacuum pump has a power of 550 watts and can create a vacuum up to -82 kPa in the system. The discharge capacity of the pump is 51 liters per minute.
3	Thermometer	Thermometers with an accuracy of 0.1°C were used to measure temperature at different points in the system.
4	Flowmeter	The flowmeter is a device that measures the volume of fluids passing through it over time. It was used to regulate the inlet flow rate to the system and to reduce errors in flow rate measurement.
5	Pressure Gauge	The barometer or pressure gauge is a device used to measure system pressure, which can measure pressure in units such as bar or millimeters of mercury.

Figure 5. Vacuum pump used in this study.

Figure 6 presents an overview of the constructed adsorption chiller system. The system consists of four main components: an evaporator, a condenser, an adsorption bed, and a vacuum pump. The condenser and adsorption bed are housed within a single chamber. Silica gel is used as the adsorbent material, which absorbs water at low temperatures and releases it into the chamber as the temperature increases. The experimental procedure in this study is as follows: Initially, all system components were thoroughly checked for leakage and proper insulation. Prior to the start of the experiment, the silica gel was dried in an oven to ensure its maximum adsorption capacity. The vacuum pump was then activated to reduce the system pressure to the desired level, creating low-pressure conditions suitable for evaporation. In the next step, hot water from a reservoir was circulated into the condenser section located within the silica gel bed. The heat caused the silica gel to desorb the absorbed water vapor, which was then condensed inside the internal condenser and expelled from the system. The flow and control of the hot water were managed manually using valves, according to the schematic diagram. Subsequently, cold water was passed through the condenser to facilitate the adsorption process. Simultaneously, a specified amount of water was introduced into the evaporator, where it evaporated under vacuum conditions. This phase change absorbed latent heat from the surroundings, thereby reducing the temperature. The resulting vapor was then adsorbed by the silica gel, completing the cycle. Throughout each stage of the experiment, the system was monitored using thermometers and pressure gauges installed at critical points. The outlet temperatures of the hot and chilled water, vacuum pressure, and ambient conditions were regularly recorded.

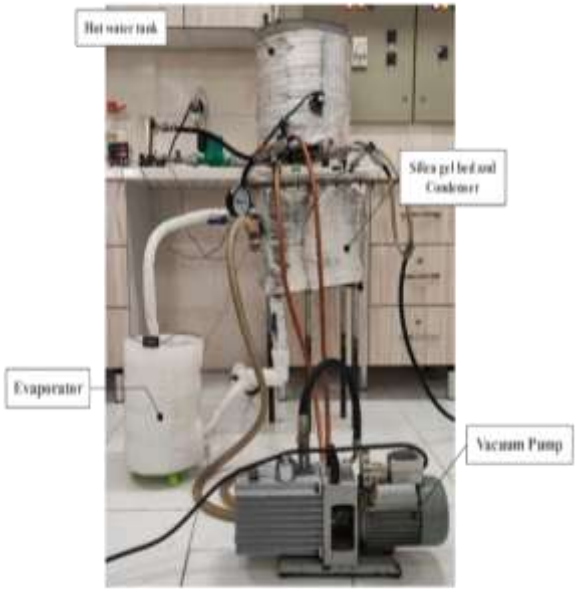

Figure 6. The constructed adsorption chiller system.

Initially, preparation is carried out in such a way that all valves are open and the entire system is evacuated. Then the evaporator valves are closed and water is injected into the chamber. The water evaporates and is absorbed by the bed. In this case, due to a slight increase in pressure, the system is evacuated again with a vacuum pump and the system is ready for testing. From this moment, the main cycle begins.

4. Results

In this section, the obtained results are analyzed. To validate the accuracy of the tests, experiments were conducted on different days. The following subsections present and discuss the results separately for each testing day.

4.1. First experiment results

Figure 7 illustrates the temperature and pressure profile of the adsorption bed over the course of the experiment. In Region 1, heating of the adsorption bed begins with a hot water flow rate of 4 liters per minute. As observed, the temperature gradually increases, reaching up to 73°C. In Region 2, the vacuum phase ends and the cooling process begins, during which the condenser flow rate is 3.6 L/min and the bed flow rate is 3.9 L/min. Region 3 marks the start of the desorption phase, with all valves closed and the hot water flow rate maintained at 4 L/min. In Region 4, the vacuum is re-established and the end valve of the evaporator is opened. The experiment is then concluded. Therefore, cooling is performed in Regions 2 and 4, resulting in a noticeable decrease in temperature.

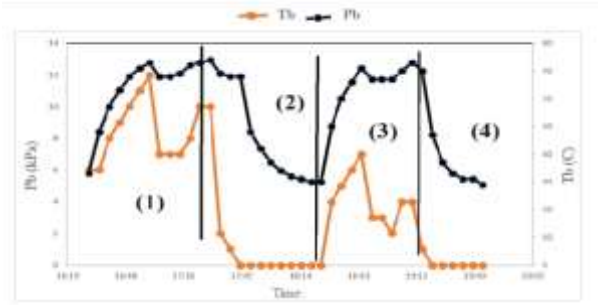

Figure 7. Temperature and pressure graph of the bed.

Figure 8 shows the temperature difference between the hot water at the inlet and outlet of the cycle. It can be observed that the maximum temperature difference in the hot water is close to 7°C. During times when the temperature difference reaches zero, the hot water entering the cycle is stopped. Additionally, at the beginning of the cycle, the temperature difference is small, but over time, approximately 1 hour into the cycle, the temperature difference increases.

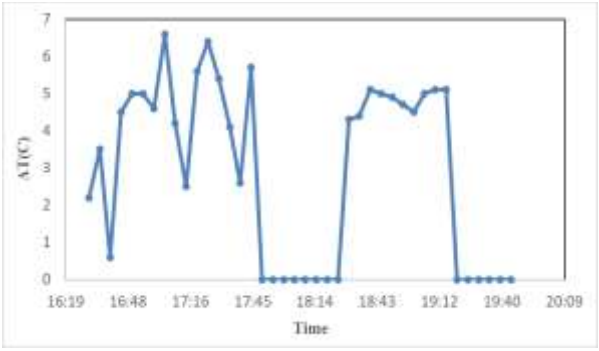

Figure 8. Temperature difference between the hot water inlet and outlet of the cycle.

Figure 9 shows the temperature difference in the cold water entering and exiting the cycle. The temperature difference in the cold water is much smaller compared to the hot water, with the maximum temperature difference reaching 3.2°C. These values are also dependent on the accuracy of the measuring instruments.

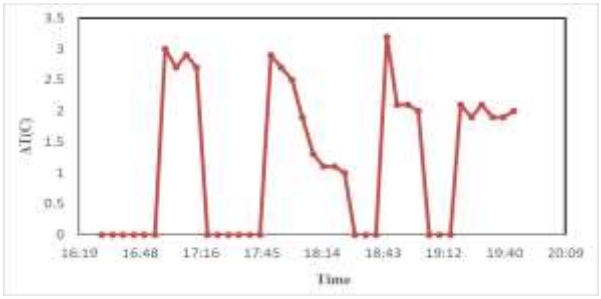

Figure 9. Temperature difference between the cold water inlet and outlet of the cycle.

Figure 10 displays the heating amount in the cycle. It can be observed that, due to the larger temperature difference created in the heating section, the amount of heat received is higher compared to the cooling section. The maximum heat received in the cycle is 1870 watts, which directly correlates with the temperature difference.

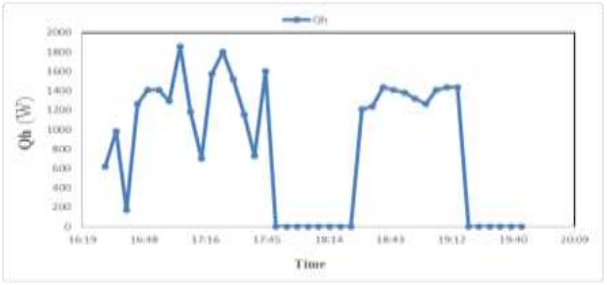

Figure 10. Amount of heating generated in the cycle.

Figure 11 shows the amount of cooling needed in the condenser section of the cycle. It is observed that, due to the smaller temperature difference in the cooling section, the amount of heat received is lower compared to the heating section. The maximum cooling achieved in the cycle is 1115 watts, which is directly related to the temperature difference.

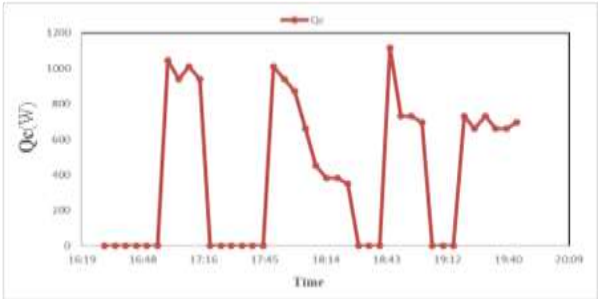

Figure 11. Amount of cooling generated in the cycle.

4.2. Second experiment results

Figure 12 shows the temperature and pressure graph of the bed on the second day of experiments. The explanations of the different regions are similar to figure 7, where the four distinct regions of the cycle are explained.

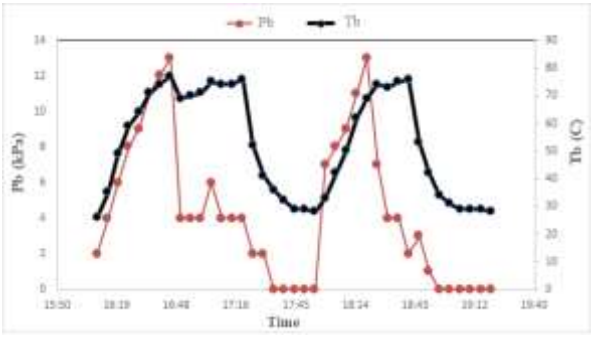

Figure 12. Temperature graph of the bed in the second experiment.

In figure 13, the temperature difference between the hot water inlet and outlet of the cycle on the second day of the experiments is shown. It is observed that the highest temperature difference in the hot water is close to 5.5°C. During times when the temperature difference reaches zero, the hot water entering the cycle is cut off. Additionally, at the beginning of the cycle, the temperature difference created is about 3.5°C, which stabilizes to a value of approximately 4.2°C after about half an hour.

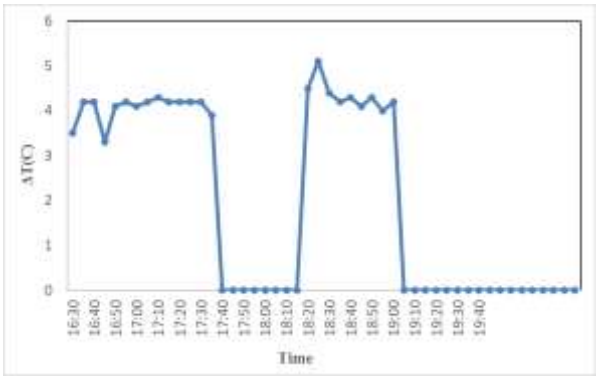

Figure 13. Temperature difference between inlet and outlet hot water in the cycle on the second day of experiments.

In figure 14, the temperature difference between the cold water inlet and outlet of the cycle on the second day of the experiments is shown. The temperature difference in the cold water is significantly less than in the hot water, and the maximum temperature difference reaches 1.1°C. These values are also dependent on the accuracy of the measuring devices. It is also observed that as the experiment progresses, the temperature difference decreases.

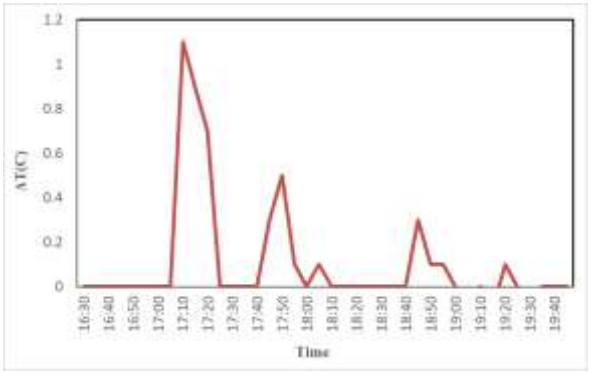

Figure 14. Temperature difference between inlet and outlet cold water in the cycle on the second day of experiments.

In figures 15 and 16, the cooling and heating amounts in the cycle on the second day of the experiments are shown. It is observed that due to the greater temperature difference in the heating section, the heat received is higher than the cooling. The highest heat received in the cycle is 1440 joules, and the highest cooling produced in the cycle is 592 joules. Another reason for the observed difference is the higher flow rate in the cooling section compared to the hot water flow, which reduces heat transfer due to the increased flow rate.

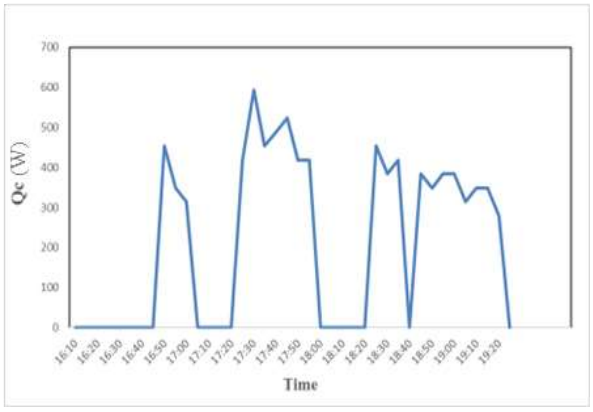

Figure 15. Amount of cooling achieved on the second day of experiments.

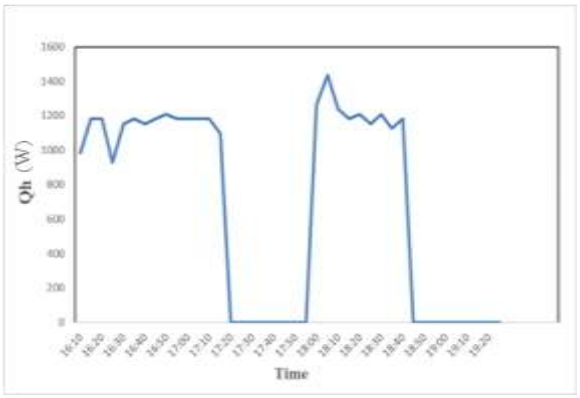

Figure 16. Amount of heating achieved on the second day of experiments.

4.3. Third experiment results

Figure 17 shows the temperature and pressure graph of the bed on the third day of experiments. The explanations for the different regions are similar to those in figure 7, where four distinct regions of the cycle are described.

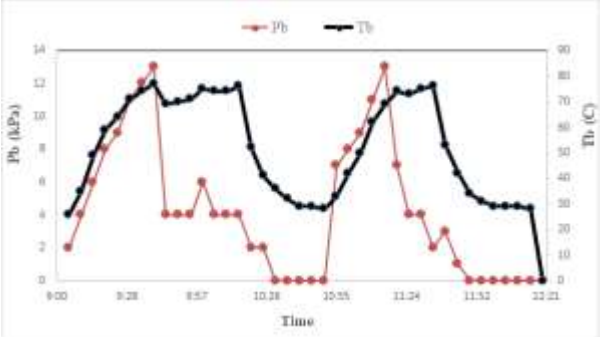

Figure 17. Temperature and pressure of the bed in the third experiment.

Figure 18 shows the temperature difference between the inlet and outlet hot water in the cycle on the third day of experiments. It can be observed that the maximum temperature difference in hot water is close to 4.5°C. When the temperature difference reaches zero, the hot water input to the cycle is cut off. Also, at the beginning of the cycle, the temperature difference is about 3.5°C, which stabilizes at around 4.5°C after about half an hour.

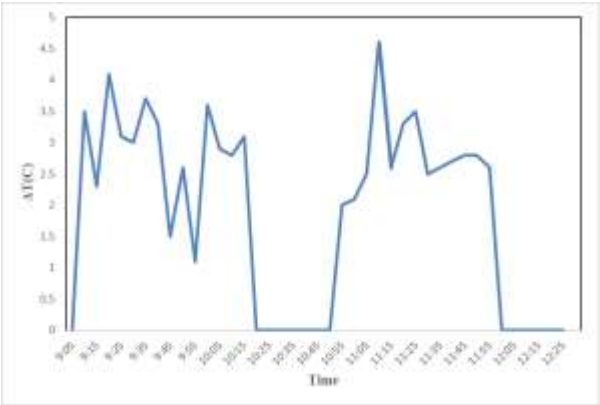

Figure 18. Temperature difference between the inlet and outlet hot water in the cycle on the third day of experiments.

Figure 19 shows the temperature difference between the inlet and outlet cold water in the cycle on the third day of experiments. The temperature difference in cold water is much lower compared to the hot water, and the maximum temperature difference reaches 1.2°C.

Figure 20 shows the amount of cooling and heating in the cycle on the third day of experiments. It can be observed that due to the greater temperature difference in the heating section, the amount of heat received is also higher compared to the cooling. The maximum heat received in the cycle is 1368 W, and the maximum cooling achieved in the cycle is 422 W. Another cause of this difference is the higher flow rate in the cooling section compared to the hot water flow.

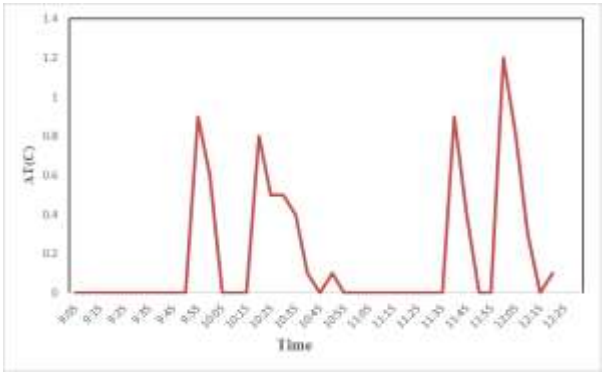

Figure 19. Temperature difference between the inlet and outlet cold water in the cycle on the third day of experiments.

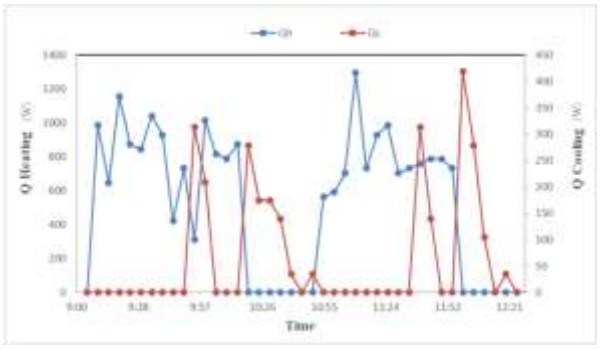

Figure 20. Amount of cooling and heating in the cycle on the third day of experiments.

Figure 21shows the COP value in the different experiments conducted. It is observed that, on average, the COP value is in the range of 0.03 to 0.05. This COP value is very low for a refrigeration system. The reason for the low COP can be due to the following reasons:

- In the ideal adsorption refrigeration cycle, the working pressure of the cycle is between 1 kPa and 4 kPa, at which the saturation temperature of water is between 7 and 28 degrees Celsius. As mentioned in the previous sections, in the current study, we achieved pressures of 2 to 15 kPa, which is far from the pressures of the ideal cycle, and the boiling temperature of water at this pressure is between 17.5 and 54 degrees Celsius.
- Among the system's shortcomings, we can mention the refrigerant passage path from the evaporator to the bed and condenser chambers, which was not properly designed to facilitate

the passage of vapor from the evaporator and absorption in the bed.

- Finally, due to the presence of the bed and condenser in a common chamber, the performance of each of which affects the boiler, the overall performance of the system has been reduced.

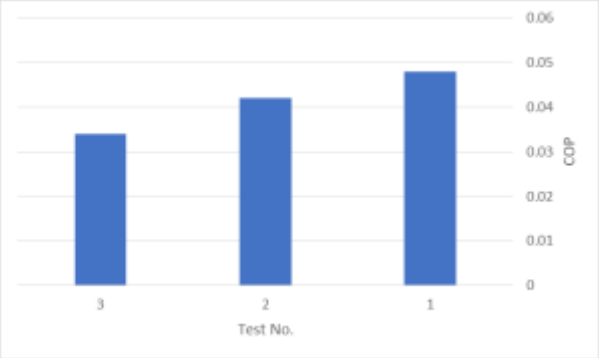

Figure 21. COP value in various experiments.

5. Conclusion

In this study, an adsorption cooling system using water and silica gel was designed, constructed, and experimentally evaluated. In the developed setup, the silica gel bed and condenser were placed within an insulated chamber, while the evaporator was positioned outside this chamber. Based on the results, the system was capable of producing a temperature difference of up to 7°C in the hot-water stream and 1.5°C in the cold-water stream. The coefficient of performance (COP) of the system was measured in three consecutive experiments as 0.048, 0.042, and 0.035, respectively. These values reflect the current operational efficiency and establish a solid foundation for further analysis and improvement. The thermal and pressure performance analysis showed that the operating pressure ranged from 2 to 15 kPa, which differs from the ideal adsorption cooling cycle range of 1 to 4 kPa. At this pressure range, the boiling point of water was between 17.5°C and 54°C, higher than the ideal saturation temperature range of 7°C to 28°C. This suggests a need for redesign to achieve more optimal conditions. In the design of the refrigerant flow path from the evaporator to the adsorption bed and condenser, the vapor flow and its adsorption mechanism were taken into account. However, further refinement of this path design could facilitate vapor flow and improve the adsorption process. Additionally, the shared chamber for the bed and condenser, which causes mutual performance interaction, plays a crucial role in the thermal behavior of the system. This design offers a valuable opportunity to study the simultaneous effects of these components on one another and can serve as a basis for future performance enhancement of the system.

6. Acknowledgment

We would like to thank the Energy Laboratory of Shahrood University of Technology for their assistance in implementing this project.

7. References

[1] Arabkoohsar, A., & Sadi, M. (2020). Technical comparison of different solar-powered absorption chiller designs for co-supply of heat and cold networks. Energy Conversion and Management, 206, 112343.

[2] Liu, Z., N. Xie, and S. Yang, Thermodynamic and parametric analysis of a coupled LiBr/H2O absorption chiller/Kalina cycle for cascade utilization of low-grade waste heat. Energy Conversion and Management, 2020. 205: p. 112370.

[3] Bellos, E., Tzivanidis, C., Symeou, C., & Antonopoulos, K. A. (2017). Energetic, exergetic and financial evaluation of a solar driven absorption chiller–A dynamic approach. Energy conversion and management, 137, 34-48.

[4] Mirzaee, M., Zare, R., Sadeghzadeh, M., Maddah, H., Ahmadi, M. H., Acıkkalp, E., & Chen, L. (2019). Thermodynamic analyses of different scenarios in a CCHP system with micro turbine–Absorption chiller, and heat exchanger. Energy Conversion and Management, 198, 111919.

[5] Rezk, A. R. M. (2012). Theoretical and experimental investigation of silica gel/water adsorption refrigeration systems (Doctoral dissertation, University of Birmingham).

[6] Younes, M.M., et al., Characterization of silica gel-based composites for adsorption cooling applications. International Journal of Refrigeration, 2020. 118: p. 345-353.

[7] Alonso, S., Morán, A., Pérez, D., Reguera, P., Díaz, I., & Domínguez, M. (2019, May). Virtual sensor based on a deep learning approach for estimating efficiency in chillers. In International Conference on Engineering Applications of Neural Networks (pp. 307-319). Cham: Springer International Publishing.

[8] Manila, M. R., Mitra, S., & Dutta, P. (2020). Studies on dynamics of two-stage air cooled water/silica gel adsorption system. Applied Thermal Engineering, 178, 115552.

[9] Sztekler, K., Kalawa, W., Mlonka-Medrala, A., Nowak, W., Mika, Ł., Krzywanski, J., ... & Debniak, M. (2020). The effect of adhesive additives on silica gel water sorption properties. Entropy, 22(3), 327.

[10] Lee, J. G., Bae, K. J., & Kwon, O. K. (2020). Performance investigation of a two-bed type adsorption chiller with various adsorbents. Energies, 13(10), 2553.

[11] Liu, Y. M., Yuan, Z. X., Wen, X., & Du, C. X. (2021). Evaluation on performance of solar adsorption cooling of silica gel and SAPO-34 zeolite. Applied Thermal Engineering, 182, 116019.

[12] Najeh, G., Gabsi, S., El Ganaoui, M., & Benelmir, R. (2021). Experimental Analysis of a Solar Adsorption System Refrigeration Cycle with Silica-Gel/Water Pair. Journal of Fundamentals of Renewable Energy and Applications, 11(1).

[13] Di, J., Wu, J. Y., Xia, Z. Z., & Wang, R. Z. (2007). Theoretical and experimental study on characteristics of a novel silica gel–water chiller under the conditions of variable heat source temperature. International Journal of Refrigeration, 30(3), 515-526.

[14] Núñez, T., Mittelbach, W., & Henning, H. M. (2007). Development of an adsorption chiller and heat pump for domestic heating and air-conditioning applications. Applied Thermal Engineering, 27(13), 2205-2212.

[15] Chen, C. J., Wang, R. Z., Xia, Z. Z., Kiplagat, J. K., & Lu, Z. S. (2010). Study on a compact silica gel–water adsorption chiller without vacuum valves: design and experimental study. Applied Energy, 87(8), 2673-2681.

[16] Chorowski, M., & Pyrka, P. (2015). Modelling and experimental investigation of an adsorption chiller using low-temperature heat from cogeneration. Energy, 92, 221-229.

[17] Pan, Q., Peng, J., & Wang, R. (2019). Experimental study of an adsorption chiller for extra low temperature waste heat utilization. Applied Thermal Engineering, 163, 114341.

[18] Chorowski, M. and P. Pyrka, Modelling and experimental investigation of an adsorption chiller using low-temperature heat from cogeneration. Energy, 2015. 92: p. 221-229.

[19] Sah, R. P., Sur, A., Sarma, N. D., & Chaurasiya, S. P. (2024). Comparative Study on Performances of Waste Heat Driven Adsorption Cooling System Using Silica Gel/Methanol and Silica Gel/Water Working Pair. Journal Européen des Systèmes Automatisés, 57(6).

[20] Du, S., Cui, Z., Wang, R. Z., Wang, H., & Pan, Q. (2024). Development and experimental study of a compact silica gel-water adsorption chiller for waste heat driven cooling in data centers. Energy Conversion and Management, 300, 117985.

[21] El-Ghetany, H. H., Omara, M. A., Abdelhady, R. G., & Abdelaziz, G. B. (2023). Design of silica gel/water adsorption chiller powered by solar energy for air conditioning applications. Journal of Energy Storage, 63, 107055.